# Nonperipheral effects in medium energy proton scattering on collective nuclear states

B. I. M. van der Cammen, A. E. L. Dieperink, and O. Scholten
*Kernfysisch Versneller Instituut, Rijksuniversiteit Groningen, 9747 AA Groningen, The Netherlands*

G. Wenes
*Los Alamos National Laboratory, Theoretical Division, MS B283 Los Alamos, New Mexico 87545*
(Received 28 July 1987)

The Glauber approximation is combined with the interacting boson model of nuclei to describe medium energy proton scattering to collective states. Channel coupling effects are included to all orders. Nonperipheral contributions are found to be nonnegligible, especially for small angles. As an illustration, cross sections for the excitation of the low lying $J^\pi=0^+$, $2^+$ states in $^{154}$Gd are presented.

## I. INTRODUCTION

Multiple excitation is conventionally described in terms of a coupled channel approach, in which only a few selected channels are treated, which are thought to be dominant. An alternative approach is possible in the interacting boson model, which provides an algebraic description of low lying collective states in open shell nuclei. Within the IBA-model space, a nonperturbative treatment of multiple excitation up to all orders is possible. In a series of papers[1,2] it was shown that this model can be used to conveniently describe the excitation of low-lying collective states in rotation-vibrational nuclei by means of medium-energy proton scattering ($E_p \sim 500-800$ MeV) in terms of the eikonal approximation.

In the past experimental studies of the (p,p') reaction on deformed nuclei focused on the excitation of the ground state band. While the angular distributions in these cases are largely determined by the geometry[1] the importance of effects arising from multiple excitation was clearly established. More recently data became available[3] on the excitation of states in side bands. These indicate that the angular distributions are sensitive to both the details of the transition densities and the coupling to other states.

The transition amplitudes as a function of the impact parameter $b$ can be expressed as an integral of the matrix elements of the exponentiated U(6) group elements $\langle \psi_f \mid \exp[f(r)G^{(\lambda)}\cdot Y^{(\lambda)}(r)] \mid \psi_i \rangle$.[1] Here the $G_\mu^{(\lambda)}$ are the infinitesimal generators of U(6) (in the coupled angular momentum representation) and the radial functions $f[(b^2+z^2)^{1/2}]$ are proportional to the collective quadrupole transitions densities $\alpha(r)$, $\beta(r)$; the latter can be obtained most directly in reactions in which the one-step excitation dominates, e.g., electron scattering.[4] Also a microscopic calculation in a shell model basis is possible.[5]

As to the reaction formalism, up to now in the eikonal approximation one simplifying assumption has been made, namely that of the peripheral approximation. In that case it appears sufficient to evaluate only the matrix elements $\langle \exp(\alpha G_\mu^{(\lambda)}) \rangle$ for $\mu=0$.[1] However, the validity of this approximation has not yet been investigated quantitatively, especially for the excitation of weaker states. For example, if we restrict ourselves to collective quadrupole vibrations, final states with odd angular momentum values can only be excited via the $\mu\neq 0$ components.

In this paper we present a more general formalism for the calculation of representation matrices of the quadrupole operator and angular distributions, which allows us to go beyond the $\mu=0$ approximation. In Sec. II the Glauber scattering formalism and the peripheral approximation are discussed. Section III is divided into a brief overview of the interacting boson model and the calculation of representation matrices in the U(5) limit. The validity of the peripheral approximation is discussed in Sec. IV, and the angular distributions for the U(5) and SU(3) limits are presented. In Sec. V our predictions are compared with recent (p,p') data for $^{154}$Gd.

## II. FORMALISM

To describe the excitation of collective states of a nucleus in proton scattering we consider the Hamiltonian

$$H=\frac{p^2}{2m}+H_T+V_{\rm int}(\mathbf{r},\hat{Q}) , \tag{2.1}$$

where $\mathbf{r}$ is the projectile coordinate, $\hat{Q}$ denotes the set of collective operators acting in the collective Hilbert space; $H_T$ is the target Hamiltonian, and $V_{\rm int}(\mathbf{r},\hat{Q})$ the coupling of the projectile to the target. It is convenient to decompose the latter in a spherical optical potential, that describes the elastic scattering on the target (in Born approximation), and a coupling of the projectile to the collective multipole degrees of freedom

$$V_{\rm int}(\mathbf{r},\hat{Q})=V_{\rm el}(r)+V_{\rm coll}(\mathbf{r},\hat{Q}) , \tag{2.2}$$

where

$$V_{\rm coll}(\mathbf{r},\hat{Q})=\sum_\lambda g_\lambda W_\lambda(r)\hat{Q}^{(\lambda)}\cdot C^{(\lambda)}(\theta,\phi) . \tag{2.3}$$

Here $\hat{Q}^{(\lambda)}$ is the collective multipole operator, $W_\lambda(r)$ its radial form factor, $g_\lambda$ its strength, and $C^{(\lambda)}(\theta,\phi)$ are the unit spherical tensors of rank $\lambda$.

 

In the impact parameter representation, the scattering amplitude can be expressed as

$$\langle J_f M_f, \mathbf{k}' \mid \hat{F} \mid J_i M_i, \mathbf{k} \rangle = \frac{k}{2\pi i} \int d^2\mathbf{b}\, e^{i\mathbf{q}\cdot\mathbf{b}} \langle J_f M_f \mid e^{-\Psi(\mathbf{b})} - 1 \mid J_i M_i \rangle \ , \tag{2.4}$$

where $\mathbf{q}=\mathbf{k}'-\mathbf{k}$ is the momentum transfer. In the eikonal approximation the profile operator $\Psi(\mathbf{b})$ takes on the form[6]

$$\Psi(\mathbf{b}) = \frac{mi}{\hbar^2 k} \sum_j \int_{-\infty}^{\infty} V(\mathbf{r}-\mathbf{r}_j) dz \ , \tag{2.5}$$

which in the $\{t\rho\}$ approximation can be written as

$$\Psi(\mathbf{b}) = -\frac{2\pi i f_0}{k} \int_{-\infty}^{\infty} dz\, \hat{\rho}(\mathbf{r}) \ , \tag{2.6a}$$

where

$$f_0 = \frac{ik}{4\pi}\sigma(1-i\beta) \equiv \frac{ik}{4\pi}\sigma_0 \tag{2.6b}$$

is the forward proton-nucleon scattering amplitude, $\sigma$ is the isospin averaged proton-nucleon cross section, and $\beta$ its ratio of real and imaginary part. It is then convenient to make a multipole decomposition of the nuclear density in terms of collective operators, analogous to Eqs. (2.2) and (2.3)

$$\hat{\rho}(\mathbf{r}) = \rho_0(r) + \sum_\lambda \rho^{(\lambda)}(r) \hat{Q}^{(\lambda)} \cdot C^{(\lambda)}(\theta,\phi) \ , \tag{2.7}$$

where $\rho_0(r)$ describes the ground state density and the $\rho^{(\lambda)}(r)$ are the multipole transition densities. This leads to a decomposition of the profile operator in two parts, $\Psi(\mathbf{b}) = \bar{\Psi}(b) + \hat{\Psi}(\mathbf{b})$, where $\bar{\Psi} \equiv \langle gs \mid \Psi \mid gs \rangle$

$$\bar{\Psi}(b) = \tfrac{1}{2}\sigma_0 \int_{-\infty}^{\infty} dz\, \rho_0(r) \tag{2.8}$$

is the elastic profile function, and $\hat{\Psi}$ describes the nuclear excitations. In the present paper we restrict ourselves to the dominant $\lambda=2$ multipole

$$\hat{\Psi}(\mathbf{b}) = \boldsymbol{\varepsilon}(\mathbf{b}) \cdot \hat{Q}^{(2)} = \sum_\mu (-)^\mu \varepsilon_{-\mu}(\mathbf{b}) \hat{Q}^{(2)}_\mu \ . \tag{2.9a}$$

Here $\boldsymbol{\varepsilon}(\mathbf{b})$ is the transition profile function for quadrupole transitions

$$\varepsilon_\mu(\mathbf{b}) = \tfrac{1}{2}\sigma_0 \int_{-\infty}^{\infty} dz\, \rho^{(2)}(r) C^{(2)}_\mu(\theta,\phi) \ . \tag{2.9b}$$

For the matrix element in Eq. (2.4) we can write

$$\langle J_f M_f \mid e^{-\Psi(\mathbf{b})} - 1 \mid J_i M_i \rangle = e^{-\bar{\Psi}(b)} \langle J_f M_f \mid e^{-\hat{\Psi}(\mathbf{b})} \mid J_i M_i \rangle - \delta_{fi} \ . \tag{2.10}$$

Here $\langle e^{-\hat{\Psi}(\mathbf{b})} \rangle$ describes the excitation to all orders. In practice we have $J_i = M_i = 0$; as a result all the factors $e^{i\mu\phi}$ from the $C^{(2)}_\mu(\theta,\phi)$ in $\varepsilon_\mu$ can be combined in a phase $\exp(iM_f\phi)$. Therefore, one can use the integral representation of the Bessel function $J_M$ to perform the azimuthal angle integration in Eq. (2.4). After inclusion of the Coulomb interaction for a spherically symmetric charge distribution $\rho_{\rm ch}(r)$, the scattering amplitude can be expressed as

$$\langle J_f M_f, \mathbf{k}' \mid \hat{F} \mid J_i = M_i = 0, \mathbf{k} \rangle = F_R(\theta)\delta_{fi} + \frac{k}{i} \int_0^\infty b\, db\, J_{|M_f|}(qb)\, e^{i\chi_{pt}(b)} (e^{-\bar{\Psi}(b)} e^{i\chi_c(b)} \langle J_f M_f \mid e^{-\hat{\Psi}(b)} \mid J_i = M_i = 0 \rangle - \delta_{fi}) \ , \tag{2.11}$$

where[7,8]

$$F_R(\theta) = -\frac{\eta}{2k \sin^2 \frac{1}{2}\theta} e^{-i\eta \ln[\sin^2(1/2)\theta] + 2i\sigma_c} \ . \tag{2.12a}$$

$$\chi_{pt}(b) = 2\eta \ln(kb) \ , \tag{2.12b}$$

$$\chi_c(b) = 8\pi\eta \int_b^\infty dt\, t^2 \rho_{\rm ch}(t) \left[ \ln \frac{1+(1-b^2/t^2)^{1/2}}{b/t} - (1-b^2/t^2)^{1/2} \right] \ . \tag{2.12c}$$

In the above equations the charge distribution, $\rho_{ch}(r)$, is normalized to unity, $\eta$ the Sommerfeld parameter

$$\eta=\frac{Ze^2}{\hbar v}\ , \tag{2.12d}$$

and

$$\sigma_c=\arg\Gamma(1+i\eta)\ . \tag{2.12e}$$

We note that now in $\hat{\Psi}(b)$: $\varepsilon_2(b)=\varepsilon_{-2}(b)$, not dependent on $\phi$. Furthermore, we rotate to a frame where $\varepsilon_{\pm1}(b)=0$.

In most applications until now, one has calculated the matrix elements in Eq. (2.10) in the so-called peripheral, or small $z/b$, approximation, which is motivated by the presence of the attenuation factor $e^{-\Psi(b)}$, that is effective for $b<R$, and the surface peaked behavior of $\varepsilon(b)$. In practice, this means that in the expansion of the $C^{(2)}_\mu(\theta,\phi)$ around $\theta=\pi/2$

$$\varepsilon_0(b)=\tfrac{1}{2}\sigma_0\int_{-\infty}^{\infty}dz\,\rho^{(2)}(r)\tfrac{1}{2}\left[-1+3\frac{z^2}{b^2}-\cdots\right],$$

$$\varepsilon_2(b)=\tfrac{1}{2}\sigma_0\int_{-\infty}^{\infty}dz\,\rho^{(2)}(r)\tfrac{1}{2}\sqrt{\tfrac{3}{2}}\left[1-\frac{z^2}{b^2}+\cdots\right], \tag{2.13}$$

only the $z=0$ term is kept. In this case the $\mu=0$ and 2 components of $\varepsilon(b)$ become proportional $\varepsilon_2(b)=-\sqrt{\frac{3}{2}}\varepsilon_0(b)$, and the matrix elements, Eq. (2.10), are easily calculated using a three dimensional rotation to a frame, where only the $\mu=0$ term of $\hat{\Psi}(b)$ survives.[1]

To get an idea about the validity of the peripheral approximation we compare in Fig. 1 the full result of $\varepsilon_\mu(b)/\sigma_0$ as a function of $b$, with that for the peripherial approximation. For $\rho^{(2)}(r)$ we took the Tassie form $\rho^{(2)}(r)\sim r(d/dr)\rho_0(r)$, with $\rho_0(r)$ of Woods-Saxon form. In order to emphasize the effect on the scattering amplitude (which is an integral over $b$) we multiplied $\varepsilon(b)$ with the attenuation factor $|e^{-\bar{\Psi}(b)}|$. One sees that the corrections to the $z=0$ approximation lead to a reduction of $\varepsilon_\mu$ (both for $\mu=0$ and $\mu=2$), as could already be expected from Eq. (2.13). Compared to the $z=0$ case the peak values of $\varepsilon_0(b)|e^{-\Psi(b)}|$ and $\varepsilon_2(b)|e^{-\bar{\Psi}(b)}|$ are reduced by 35% and 12%, respectively. As a consequence, for small $q$ values, the scattering amplitude, Eq. (2.11) is approximately reduced by the same amount. On the other hand, it can be shown[9] by expanding the spherical tensors $C^{(2)}_\mu$ in terms of powers of $z^2/b^2$ [see Eq. (2.13)] and the use of the stationary phase approximation that with increasing $q$ the corrections to the $z=0$ approximation decrease as $(b_0q)^{-2/3}$. This effect can also be seen by comparing Figs. 2 and 3. We also note that in the full calculation $\varepsilon_0$ and $\varepsilon_2$ no longer have the same dependence on $b$, which will break the proportionality of the $M=0$ and $M=2$ transition matrix elements (see Sec. III B).

From Eq. (2.11) it is clear that the nuclear structure information is contained in the matrix elements $\langle J_fM_f|e^{-\hat{\Psi}}|J_i=M_i=0\rangle$. In the next section we evaluate these matrix elements for the interaction boson approximation (IBA) model.

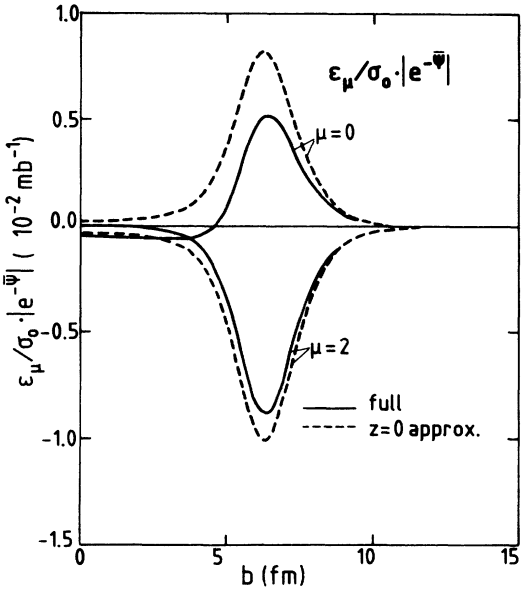


FIG. 1. The functions $\varepsilon_\mu(b)/\sigma_0$ ($\mu=0,2$) multiplied with the attenuation factor $|e^{-\bar{\Psi}(b)}|$ are plotted as a function of $b$. The full result is given by the solid line and the $z=0$ approximation by the dashed line.

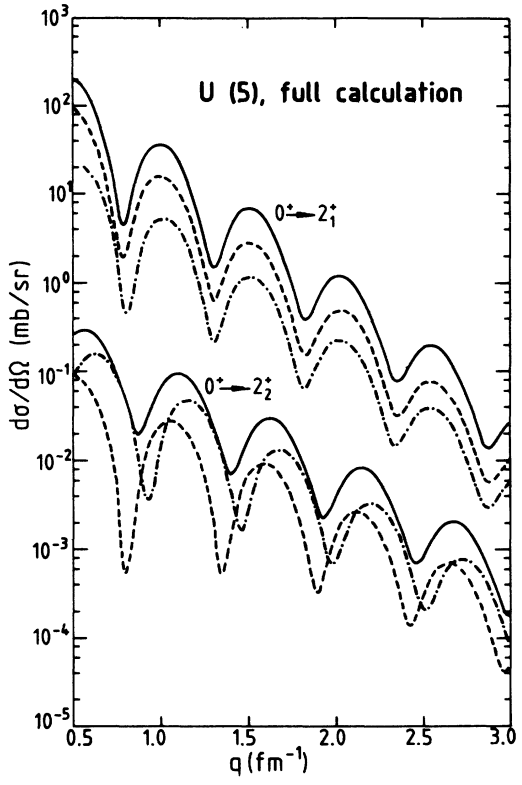


FIG. 2. The angular distributions for the excitation of the $2_1^+$ and $2_2^+$ states in the U(5) limit for the full calculation (solid curves). The contribution of the $M=0$ and 2 substates are represented by the dashed-dotted and the dashed curves, respectively.

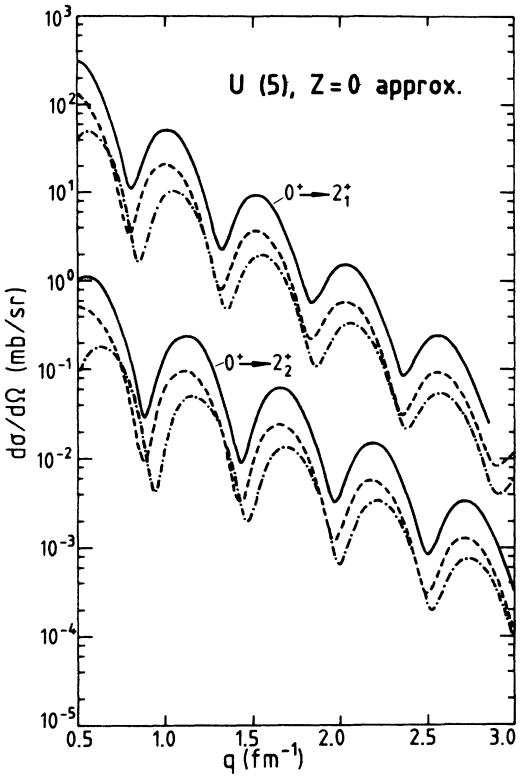


FIG. 3. Same as in Fig. 2, for the peripheral approximation.

## III. NUCLEAR STRUCTURE INFORMATION

In this section we concentrate on the nuclear structure aspects. This degree of freedom is described in the framework of the IBA model discussed in Sec. III A. The representation matrices for U(5) basis states of the IBA model will be evaluated in Sec. III B. This is done by decomposing the initial and final states in Eq. (2.11) in the $M$ scheme, and for the $N=1$ or single-boson representation matrices using the results of the Appendix. We will also discuss the validity of the peripheral approximation in the transition matrix elements.

### A. The IBA model

In this paper we will make use of the IBA model[10] to describe the collective excitations of the target nucleus in terms of $s$ ($L=0$) and $d$ ($L=2$) bosons. In the framework of this model, the excitation spectrum and the according wave functions are determined by the Hamiltonian

$$H=\varepsilon_d \hat{n}_d+\kappa \hat{Q}^{(2)}\cdot\hat{Q}^{(2)}+\kappa' \hat{L}^{(1)}\cdot\hat{L}^{(1)} , \tag{3.1}$$

where $\hat{n}_d=\sum_\mu d_\mu^\dagger d_\mu$ is the $d$-boson number operator and $\hat{Q}^{(2)}$ is the quadrupole operator

$$\hat{Q}_\mu^{(2)}=(s^\dagger \tilde{d}+d^\dagger s)_\mu^{(2)}+\chi(d^\dagger \tilde{d})_\mu^{(2)} . \tag{3.2}$$

The first term in the Hamiltonian Eq. (3.1) represents the single-boson energies ($\varepsilon_d$ is the energy difference between $d$ and $s$ bosons), whereas the second describes the quadrupole interaction (with strength $\kappa$). In the following the $\hat{L}\cdot\hat{L}$ term can be dropped, because it does not affect the wave functions. By appropriate choice of the parameters $\varepsilon_d$, $\kappa$, and $\chi$, the IBA model is able to describe vibrational and rotational nuclei, as well as nuclei in the transitional region.

In general, the nuclear eigenstates are obtained by diagonalization of $H$ in the U(5) basis, which means that the states are labeled by the quantum numbers of the U(5) group chain

$$\underset{[N]}{U(6)} \supset \underset{n_d}{U(5)} \supset \underset{\tau\ (n_\Delta)}{O(5)} \supset \underset{L}{O(3)} \supset \underset{M}{O(2)} , \tag{3.3}$$

$$|N,n_d,\tau,n_\Delta,L,M\rangle=\eta_{N,n_d,\tau}(s^\dagger)^{N-n_d}(d^\dagger\cdot d^\dagger)^{1/2(n_d-\tau)}|N=n_d=\tau,n_\Delta,L,M\rangle . \tag{3.4}$$

For the calculation of the representation matrices, we allow for the $(s^\dagger\tilde{d}+d^\dagger s)$ and the $(d^\dagger\tilde{d})^2$ term in the quadrupole operator in Eq. (2.9) two different radial form factors $\alpha(r)$ and $\beta(r)$, resulting in two different transition profile functions $\varepsilon_\mu(\mathbf{b})$ and $\eta_\mu(\mathbf{b})$

$$\hat{\Psi}(\mathbf{b})=\varepsilon(\mathbf{b})\cdot(d^\dagger s+s^\dagger\tilde{d})^{(2)}+\eta(\mathbf{b})\cdot(d^\dagger\tilde{d})^{(2)} , \tag{3.5}$$

$$\varepsilon_\mu(\mathbf{b})=\tfrac{1}{2}\sigma_0\int_{-\infty}^{\infty} dz\,\alpha(r)C_\mu^{(2)}(\theta,\phi) , \tag{3.6a}$$

$$\eta_\mu(\mathbf{b})=\tfrac{1}{2}\sigma_0\int_{-\infty}^{\infty} dz\,\beta(r)C_\mu^{(2)}(\theta,\phi) . \tag{3.6b}$$

The form factors $\alpha(r)$ and $\beta(r)$ can be determined from electron scattering. For hadron scattering, these form factors have to be multiplied with a hadronic factor, discussed in Sec. V. After determination of $\hat{\Psi}$, the transition matrix, Eq. (2.10), can, in principle, be calculated in closed form, as is discussed below.

### B. Representation matrices for U(5) basis states

For $N=1$ the representation matrices to be calculated are of the form

$$\langle s,d_{\mu'}|e^{-\hat{\Psi}}|s,d_\mu\rangle . \tag{3.7}$$

In the Appendix they are evaluated in closed form by diagonalizing the operator $\hat{\Psi}$ in the basis $\{|d_\mu\rangle,|s\rangle\}$.

In the special case that $\chi=0$ (hence $\eta_\mu=0$) the representation matrices for $N=1$ reduce to

$$\langle d_\mu|\hat{U}|s\rangle=-\frac{\varepsilon_\mu}{\lambda}\sinh\lambda\equiv\beta_\mu , \tag{3.8a}$$

$$\langle s|\hat{U}|s\rangle=\cosh\lambda\equiv\alpha , \tag{3.8b}$$

where we have defined

$$\hat{U}=\exp(-\hat{\Psi}) , \tag{3.8c}$$

$$\lambda=(\varepsilon_0^2+2\varepsilon_2^2)^{1/2} . \tag{3.8d}$$

With these results the representation matrices for general $N$ in the U(5) basis (for $\chi=0$) can easily be evaluated. First, the decomposition of the U(5) many-boson ground state is given by

$$|s^N\rangle=\frac{1}{\sqrt{N!}}(s^\dagger)^N|0\rangle ,$$

from which it follows

$$\hat{U}|s^N\rangle=\frac{1}{\sqrt{N!}}(\hat{U}s^\dagger\hat{U}^{-1})^N|0\rangle$$
$$=\frac{1}{\sqrt{N!}}(\alpha s^\dagger+\beta\cdot d^\dagger)^N|0\rangle . \tag{3.9}$$

With this result the many-boson transition matrix from the ground state to an excited state can be written as

$$\langle[N],n_d,\tau,n_\Delta,JM\,|\,\hat{U}\,|\,[N],n_d=\tau=n_\Delta=J=M=0\rangle$$
$$=\frac{\sqrt{N!}}{n_d!}\eta_{Nn_d\tau}\alpha^{N-n_d}\langle[\tau],\tau\tau n_\Delta,JM\,|\,(\tilde{d}\cdot\tilde{d})^{1/2(n_d-\tau)}(\beta\cdot d^\dagger)^{n_d}\,|\,0\rangle . \tag{3.10}$$

The normalization coefficient $\eta_{Nn_d\tau}$ (Ref. 11) is given by

$$\eta_{Nn_d\tau}=\left[\frac{(2\tau+3)!!}{(N-n_d)!(\tau+n_d+3)!!(n_d-\tau)!!}\right]^{1/2} . \tag{3.11}$$

After some algebra we find for the transition matrix

$$\langle[N],n_d,\tau,n_\Delta,J,M\,|\,\hat{U}\,|\,[N],n_d=\tau=n_\Delta=J=M=0\rangle=\sqrt{N!}\eta_{Nn_d\tau}\alpha^{N-n_d}(\beta\cdot\beta)^{1/2(n_d-\tau)}B_{\tau,n_\Delta,J,M}(\beta_0,\beta_2) , \tag{3.12a}$$

where the function $B_{\tau,n_\Delta,J,M}(\beta_0,\beta_2)$ is given by

$$B_{\tau,n_\Delta,J,M}(\beta_0,\beta_2)=\frac{\langle[\tau],\tau_\Delta\tau,n,J,M\,|\,(\beta\cdot d^\dagger)^\tau\,|\,0\rangle}{\tau!} . \tag{3.12b}$$

The functions $B$ are given in Table I for the lowest values of $\tau$.

To illustrate the influence of the peripheral approximation we evaluate expression (3.10) for some special cases.

(a) Elastic scattering:

$$\langle 0_1^+\,|\,\hat{U}\,|\,0_1^+\rangle=\langle[N],n_d=\tau=n_\Delta=J=M=0\,|\,\hat{U}\,|\,[N],n_d=\tau=n_\Delta=J=M=0\rangle=(\cosh\lambda)^N . \tag{3.13}$$

Since to lowest order $\hat{\Psi}$ does not contribute to the elastic scattering matrix element, the influence of the $z=0$ approximation is negligible.

(b) First $L^\pi=2^+$ state:

$$\langle 2_1^+,M\,|\,\hat{U}\,|\,0_1^+\rangle=\langle[N],n_d=\tau=1,n_\Delta=0,J=2,M\,|\,\hat{U}\,|\,[N],n_d=\tau=n_\Delta=J=M=0\rangle=\sqrt{N}\,(\cosh\lambda)^{N-1}\frac{\varepsilon_M}{\lambda}\sinh\lambda . \tag{3.14}$$

The result (3.14) shows that the matrix elements for $M=0$ and 2 are independent, whereas in the peripheral approximation the $M=0$ and 2 components of the matrix element are related by

$$\langle 2_1^+,M=2\,|\,\hat{U}\,|\,0_1^+\rangle=-\sqrt{\tfrac{3}{2}}\langle 2_1^+,M=0\,|\,\hat{U}\,|\,0_1^+\rangle . \tag{3.15}$$

(c) Second $L^\pi=2^+$ state:

$$\langle 2_2^+,M\,|\,\hat{U}\,|\,0_1^+\rangle=\langle[N],n_d=\tau=2,n_\Delta=0,J=2,M\,|\,\hat{U}\,|\,[N],n_d=\tau=n_\Delta=J=M=0\rangle$$
$$=\begin{cases}\sqrt{N(N-1)}\alpha^{N-2}\cdot 2\sqrt{\frac{1}{7}}\beta_0\beta_M & (M=\pm 2) ,\\ \sqrt{N(N-1)}\alpha^{N-2}\sqrt{\frac{1}{7}}(\beta_0^2-2\beta_2\beta_{-2}) & (M=0) .\end{cases} \tag{3.16}$$

In this case the $z=0$ approximation is less adequate than above, since because of the second order character of the transitions, the corrections are now quadratic. In particular, we see that the absolute value of the $M=0$ transition element can easily be larger than the one for $M=2$, in contrast to the peripheral approximation, where the relation (3.15) holds.

(d) First $L^\pi=3^+$ state:

$$\langle 3_1^+,M\,|\,\hat{U}\,|\,0_1^+\rangle=\langle[N],n_d=\tau=3,n_\Delta=0,J=2,M\,|\,\hat{U}\,|\,[N],n_d=\tau=n_\Delta=J=M=0\rangle$$
$$=\sqrt{N(N-1)(N-2)}\alpha^{N-3}\frac{1}{\sqrt{30}}(3\beta_0^2\beta_M-2\beta_M^2\beta_{-M})\cdot\delta_{|M|,2} . \tag{3.17}$$

TABLE I. The function $B_{\tau,n_\Delta,J,M}(\beta_0,\beta_2)$ [see Eq. (3.12b)] for the lowest values of $\tau$.

| $\tau$ | $n_\Delta$ | $J$ | $M$ | $B(\beta_0,\beta_2)$ |
|---|---|---|---|---|
| 0 | 0 | 0 | 0 | 1 |
| 1 | 0 | 2 | 0 | $\beta_0$ |
| | | | 2 | $\beta_2$ |
| 2 | 0 | 2 | 0 | $\sqrt{\frac{1}{7}}(\beta_0^2-2\beta_2\beta_{-2})$ |
| | | | 2 | $2\sqrt{\frac{1}{7}}\beta_0\beta_2$ |
| 2 | 0 | 4 | 0 | $\sqrt{\frac{1}{35}}(3\beta_0^2+\beta_2\beta_{-2})$ |
| | | | 2 | $\sqrt{\frac{3}{7}}\beta_0\beta_2$ |
| | | | 4 | $\sqrt{\frac{1}{2}}\beta_2^2$ |
| 3 | 0 | 3 | 0 | 0 |
| | | | 2 | $\sqrt{\frac{1}{30}}(3\beta_0^2\beta_2-2\beta_2^2\beta_{-2})$ |

Clearly, this element vanishes in the peripheral approximation, where $\beta_2=-\sqrt{\frac{3}{2}}\beta_0$. The reason for this as well as for the vanishing population of the $M=0$ substate in the full calculation is that a symmetric $L=3$ state of three identical phonons ($d$ bosons) cannot be constructed out of $d_0$ bosons only. In the next section we will discuss how the differences in the transition matrix elements due to the $z=0$ approximation affect the cross section.

## IV. CROSS SECTIONS FOR LIMITING CASES

In order to illustrate the sensitivity of the nonperipheral effects to details of the nuclear structure, we present cross sections for proton scattering on nuclei in two IBA limits: U(5) and SU(3).

As parameters we used the following: the nuclear density is parametrized by a Fermi distribution with radius $R=1.07A^{1/3}$ (fm) and thickness $a=0.68$ fm. For the structure functions in Eq. (3.6) we use $\alpha(r)=\lambda_2 r(d/dr)\rho_0(r)$ (the Tassie form) and $\beta(r)=\lambda_2' r^2(d^2/dr^2)\rho_0(r)$. They are normalized such that $\int \alpha(r)r^4dr=e_B$ (the boson effective charge) and

$$\frac{\int dr\, r^4\beta(r)}{\int dr\, r^4\alpha(r)}=\chi\ . \tag{4.1}$$

This yields $\lambda_2'=-\frac{1}{6}\lambda_2\chi$. Furthermore, $E_{\rm kin}=800$ MeV, and for the elementary proton-nucleon cross section, we took the isospin average of the Arndt data[12]: $\sigma=41$ mb, $\beta=-0.17$.

### A. The U(5) limit

To illustrate the U(5) limit, we take $\chi=0$, $N=8$, and $\lambda_2$ in such a way as to reproduce $B(E2,0_1^+\rightarrow 2_1^+)$ in $^{148}$Sm.

In Fig. 2 we plot for the first $2^+$ state the total differential cross section as well as the contribution of the angular momentum projections $M_f=0$ and $M_f=2$ separately. Also drawn are the cross sections in the peripheral approximation (Fig. 3). It is seen that the correction to the peripheral approximation leads to a reduction of the cross sections for both the $M=0$ and $M=2$ substrates. The effect is larger for the $M=0$ substrate than for the $M=2$ substate, since the correction to $\varepsilon_0(b)$ is larger than to $\varepsilon_2(b)$. Also, the correction causes a shift in the location of the minima and maxima of the cross sections to smaller values. This shift is larger for $M=0$ than for $M=2$, and due to interference effects, this leads to slightly deeper minima of the total cross sections.

The calculated cross sections for the excitation to the second $2^+$ state, shown in Figs. 2 and 3, show that the correction to the peripheral approximation is much larger than for the $2_1^+$ state. The reason is that now at least two step processes have to take place, whereas the excitation of the $2_1^+$ state proceeds to a large extent via a one step process. Furthermore, we note that the cross sections are dominated by the $M=0$ part, in contrast to the situation in the $z=0$ approximation. This can be explained by the fact that in the matrix element Eq. (3.16), $\beta_2\sim-1.7\beta_0$ (see Fig. 1) compared to $\beta_2=-\sqrt{\frac{3}{2}}\beta_0$ for the peripheral approximation.

Of special interest is the excitation of the first $3^+$ state, shown in Fig. 4. In the peripheral approximation, the cross section to states with odd $L$ vanishes and therefore its excitation strength is a direct measure of the importance of nonperipheral effects.

### B. The SU(3) limit

To investigate this limit, we added a small symmetry breaking term to the Hamiltonian of the pure SU(3) limit to split the degeneracy of the second and third $2^+$ states. We take $\chi=-\frac{1}{2}\sqrt{7}$, and $\lambda_2$ such as to reproduce the $B(E2,0_1^+\rightarrow 2_1^+)$ in $^{154}$Sm. Although multistep contributions are larger than in the U(5) limit, the cross sections for the first $2^+$ state (Fig. 5) are similar to the ones for the U(5) limit. For the $2_\beta^+$ and $2_\gamma^+$ states, there is not only an

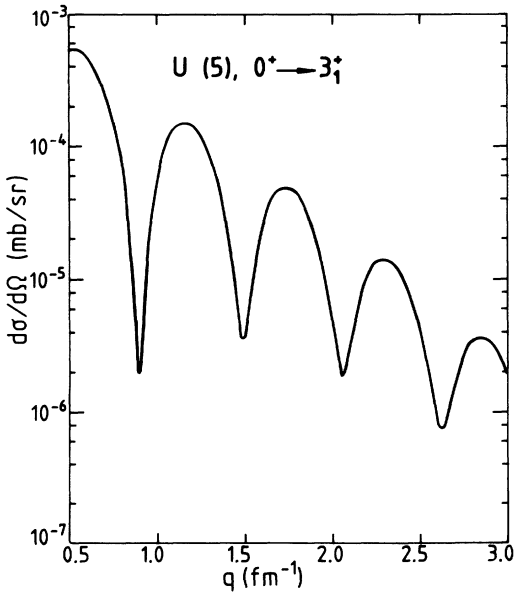


FIG. 4. The differential cross section for the excitation of the $3_1^+$ state in the U(5) limit.

overall reduction of the cross sections compared to the $z=0$ approximation, but also a shift in the position of the minima and maxima. Furthermore, it is found that the $2_\gamma^+$ state is dominated by the $M=2$ contribution, in contrast to the $2_2^+$ state in U(5). This is caused by the $(d^\dagger d)^{(2)}$ term in the quadrupole operator, which gives rise to one-step contributions.

## V. RESULTS FOR $^{154}$Gd

In this section we compare the calculated cross sections and data,[3,13] for different $2^+$ states in $^{154}$Gd. The eigenstates are calculated in program PHINT.[14] The parameters used are $N=7$, $\varepsilon_d=0.35$, $\kappa=-0.44$, $\chi=-1.3$, $\kappa'=0.002$ [see Eqs. (3.1) and (3.2)]. They were chosen in such a way to reproduce the energies of the $2_1^+$, $2_2^+$, $2_3^+$, and $6_1^+$ states.

The strength $\lambda_2$ of the structure functions can be obtained from the experimental $B(E2)$ values of Gd. This value should be multiplied with a hadronic factor, because hadronic probes also interact directly with neutrons. This factor is approximately equal to 2.[2] The quadrupole operator is given by

$$\hat{Q}_\mu^{(2)} = \left[\frac{4\pi}{5}\right]^{1/2} \int_0^\infty dr\, r^4 [\alpha(r)(s^\dagger \tilde{d} + d^\dagger s)_\mu^{(2)} + \beta(r)(d^\dagger \tilde{d})_\mu^{(2)}]$$
$$= \left[\frac{4\pi}{5}\right]^{1/2} \left[\int_0^\infty dr\, r^4 \alpha(r)\right] \times [(s^\dagger \tilde{d} + d^\dagger s) + \chi(d^\dagger \tilde{d})]_\mu^{(2)} , \tag{5.1}$$

where in the last step we used normalization condition (4.1). The $B(E2)$ for this quadrupole operator can be calculated using program FBEM (Ref. 14) (parameter $\chi=-1.5$). Normalization to experimental values yields $\lambda_2=-0.022$. Following the Arndt phase shift analysis[12] for the experimental proton energy, $E_k=646$ MeV, we take $\sigma=39.8+i(6.8)$ for the isospin average of the proton-nucleon cross section. The other parameters used have the same values as in Sec. IV.

The best fit for the GD data[13] for excitation to the $2_{gs}^+$ state is obtained for $\lambda_2=-0.02$, which is about 10% lower in magnitude than the result of the $B(E2)$ calculation.

As can be seen from Fig. 6, the agreement with the data is good for the $2_{gs}^+$ state, and reasonable for the $2_\gamma^+$ state. A possible explanation for the discrepancies in the $2_\gamma^+$ cross section is that $F$-spin admixtures play a role in the nonyrast states of $^{154}$Gd as suggested in Ref. 15. This means that for these states the neutron and proton transition densities are not proportional as assumed in the present work.

## VI. CONCLUSIONS

In this paper transition matrix elements and angular distributions were calculated to all orders, using the Glauber approximation. It was found that corrections to the peripheral (or $z=0$) approximation can give rise to large effects in the excitation of side bands, especially in the angular momentum projections of the angular distributions.

We compared our calculations with (p,p') data for the $2_{gs}^+$ and $2_\gamma^+$ states in $^{154}$Gd and obtained good results with one and the same parameter set.

## ACKNOWLEDGMENTS

We would like to thank R. Bijker and J. N. Ginocchio for useful discussions, and N. M. Hintz for making the data available to us prior to publication. This work has

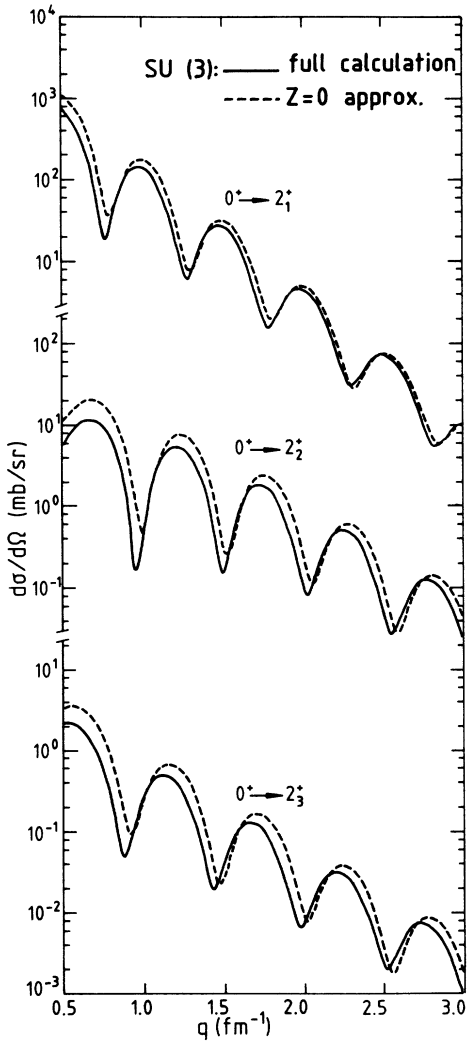


FIG. 5. The angular distributions for the excitation of the first three $2^+$ states in the SU(3) limit. The solid line is for the full calculation and the dashed line for the peripheral approximation.

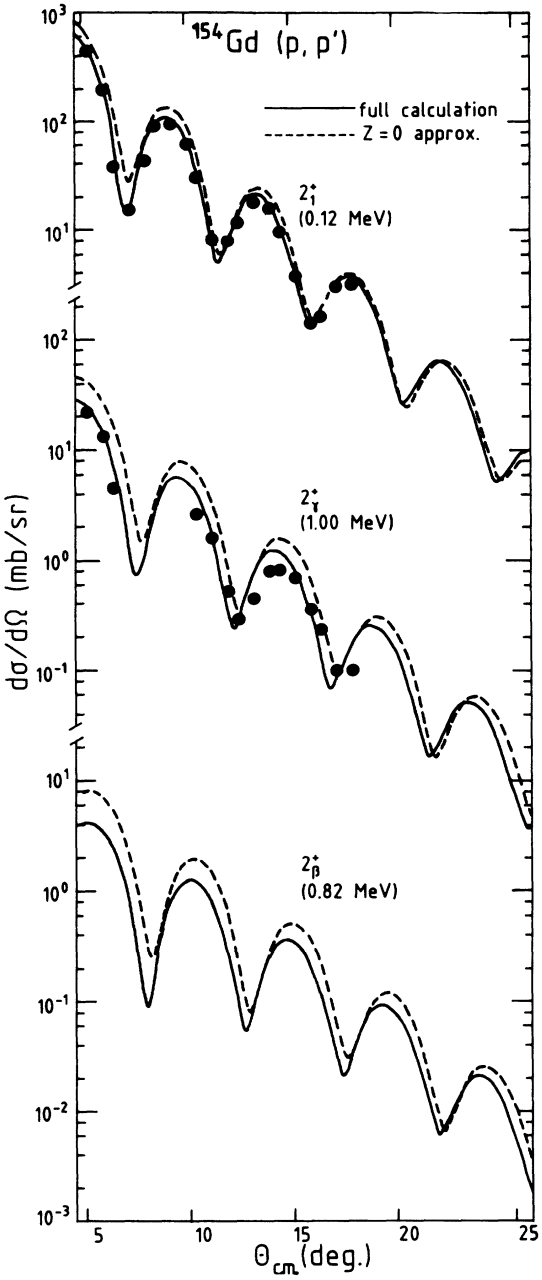


FIG. 6. The calculated angular distributions for the excitation of $2_1^+$, $2_\beta^+$, and $2_\gamma^+$ states in $^{154}$Gd. The full calculation is shown by the solid line, and the $z=0$ approximation by the dashed line. The data are taken from Ref. 13.

been performed as part of the research program of "Stichting voor Fundamenteel Onderzoek der Materie" (FOM) which is financially supported by the "Organisatie voor Zuiver Wetenschappelijk Onderzoek" (ZWO). We also acknowledge support by the NATO International Collaboration Grant RG 85/0036 and by the U.S. Department of Energy.

## APPENDIX: REPRESENTATION MATRIX FOR A SINGLE BOSON

In this appendix the matrix elements of the operator $e^{-\hat{\Psi}}$ with $\hat{\Psi}$ from Eq. (3.5) are calculated. This will be done through diagonalization of $\hat{\Psi}$ with respect to basis $\{|d_2\rangle, |d_0\rangle, |d_{-2}\rangle, |s\rangle; |d_1\rangle, |d_{-1}\rangle\} = \{|\text{even}\rangle; |\text{odd}\rangle\}$. First we note that in Eq. (3.5) the $\mu=\pm1$ terms are not present and therefore the $d_{\pm1}$ basis states do not couple to the others; therefore, we can write $\hat{\Psi}=\hat{\Psi}_{\text{even}}\times\hat{\Psi}_{\text{odd}}$, where

$$\hat{\Psi}_{\text{even}}=\begin{bmatrix}\eta_0 & \eta_2 & 0 & \varepsilon_2\\ \eta_2 & -\eta_0 & \eta_2 & \varepsilon_0\\ 0 & \eta_2 & \eta_0 & \varepsilon_2\\ \varepsilon_2 & \varepsilon_0 & \varepsilon_2 & 0\end{bmatrix}, \tag{A1a}$$

$$\hat{\Psi}_{\text{odd}}=\begin{bmatrix}-\frac{1}{2}\eta_0 & \sqrt{\frac{3}{2}}\eta_2\\ \sqrt{\frac{3}{2}}\eta_2 & -\frac{1}{2}\eta_0\end{bmatrix}. \tag{A1b}$$

We have absorbed a factor $\sqrt{\frac{2}{7}}$ in all $\eta_\mu$ to simplify the notation. For the $4\times4$ sector $\hat{\Psi}_{\text{even}}$ the eigenvalue $\eta_0$ is readily found and the transformation

$$|d_{\pm2}\rangle\rightarrow\frac{1}{\sqrt{2}}|d_2\pm d_{-2}\rangle$$

leads to a $3\times3$ matrix that can be diagonalized in closed form. The solution of the eigenvalue equation

$$\lambda^3+a_2\lambda+a_3=0, \tag{A2a}$$

where

$$a_2=-(\varepsilon_0^2+2\varepsilon_2^2+\eta_0^2+2\eta_2^2);$$

$$a_3=-[4\varepsilon_0\varepsilon_2\eta_2+(2\varepsilon_2^2-\varepsilon_0^2)\eta_0] \tag{A2b}$$

can be expressed in the form[16]

$$\lambda_k=e^{(2/3)(k-1)\pi i}P+e^{(-2/3)(k-1)\pi i}P^* \quad (k=1,2,3), \tag{A3a}$$

where

$$P=\left[-\tfrac{1}{2}a_3+i\left[-\frac{a_2^3}{27}-\frac{a_3^2}{4}\right]^{1/2}\right]^{1/3}. \tag{A3b}$$

Now also $\hat{U}_{\text{even}}=\exp(-\hat{\Psi}_{\text{even}})$ is diagonal in the basis $|\mathbf{k},4\rangle$, consisting of the eigenvectors of $\hat{\Psi}_{\text{even}}$, where (before normalization)

$$|\mathbf{k}\rangle=(\varepsilon_2\lambda_k+\varepsilon_2\eta_0+\varepsilon_0\eta_2)|d_2+d_{-2}\rangle +(\varepsilon_0\lambda_k+2\varepsilon_2\eta_2-\varepsilon_0\eta_0)|d_0\rangle+(\lambda_k^2-\eta_0^2-2\eta_2^2)|s\rangle, \tag{A4a}$$

$$|4\rangle=|d_2-d_{-2}\rangle. \tag{A4b}$$

The eigenvalues of $\hat{U}_{\text{even}}$ are $\exp(-\lambda_k)$ and $\exp(-\eta_0)$, respectively.

[1]J. N. Ginocchio, in *Proceedings of the International Workshop on Interacting Boson-Boson and Boson-Fermion Systems,* editded by O. Scholten (World-Scientific, Singapore, 1984), p. 315; R. D. Amado, J. A. McNeil, and D. A. Sparrow, Phys. Rev. C **25**, 13 (1982).

[2]J. N. Ginochio, Nucl. Phys. **A421**, 369c (1984); G. Wenes, J. N. Ginocchio, A. E. L. Dieperink, and B. van der Cammen, *ibid.* **459**, 631 (1986).

[3]J. N. Ginocchio, G. Wenes, R. D. Amado, D. C. Cook, N. M. Hintz, and M. M. Gazzaly, Phys. Rev. C **36**, 2436 (1987).

[4]M. A. Moinester *et al.*, Nucl. Phys. **A383**, 264 (1982).

[5]O. Scholten, in Ref. 1, p. 260.

[6]R. J. Glauber, in *Lectures in Theoretical Physics,* edited by W. E. Britten and L. G. Burham (Interscience, New York, 1959).

[7]I. Ahmad, Nucl. Phys. **A247**, 418 (1975)

[8]R. M. Ikeda and J. A. McNeil, Phys. Rev. C **24**, 2754 (1981).

[9]R. D. Amado, F. Lenz, J. A. McNeil, and D. A. Sparrow, Phys. Rev. C **22**, 2094 (1980).

[10]A. Arima and F. Iachello, Ann. Phys. **99**, 253 (1976); **111**, 201 (1978); **123**, 468 (1979).

[11]G. Wenes, N. Yoshinaga, and A. E. L. Dieperink, Nucl. Phys. **A443**, 472 (1985).

[12]S. J. Wallace, Adv. Nucl. Phys. **12**, 135 (1981); R. A. Arndt, Program SAID, Virginia Polytechnic Institute and State University, 1984 (unpublished).

[13]N. M. Hintz and D. C. Cook (private communication).

[14]O. Scholten, program package PHINT, University of Groningen (unpublished).

[15]T. Otsuka, G. Wenes, and J. N. Ginocchio, Los Alamos National Laboratory Report LA-UR-87-2488, 1987 (unpublished).

[16]G. Rosensteel and D. J. Rowe, Ann. Phys. **104**, 135 (1977).